Available online at www.sciencedirect.com
SCIENCE DIRECT®
European Journal of Medicinal Chemistry 40 (2005) 674–686
EUROPEAN JOURNAL OF MEDICINAL CHEMISTRY
www.elsevier.com/locate/ejmech

Aromatic–aromatic and proline–aromatic interactions in endomorphin-1 and endomorphin-2

Balázs Leitgeb [a,b,*], Géza Tóth [a]

[a] *Institute of Biochemistry, Biological Research Center of the Hungarian Academy of Sciences, Temesvári krt. 62, H-6726 Szeged, Hungary*
[b] *Institute of Biophysics, Biological Research Center of the Hungarian Academy of Sciences, Temesvári krt. 62, H-6726 Szeged, Hungary*

Received 14 October 2004; revised and accepted 21 October 2004

Available online 24 March 2005

Abstract

We investigated the aromatic–aromatic and proline–aromatic interactions in endomorphin-1 and endomorphin-2, and different types of these interactions were observed. For all the interacting pairs, the preferred geometric orientations were identified. We examined these interactions in the preferred secondary structures, which are different types of β-turns and γ-turns. These results revealed that the majority of the turn structures contained one of the interacting aromatic–aromatic or proline–aromatic pairs. On the basis of our results, it can be assumed that these interactions may be important in the determination and stabilization of the structures of endomorphins. Furthermore, our observations suggest that a conformation stabilized by an aromatic–aromatic or proline–aromatic interaction can play an important role in the association with the receptor.

Keywords: Endomorphin; Conformational analysis; Aromatic–aromatic interaction; Proline–aromatic interaction; β-Turn; γ-Turn

1. Introduction

Aromatic–aromatic interactions between different aromatic amino acids (Phe, Tyr and Trp) are important noncovalent interactions in proteins and peptides. The aromatic–aromatic interactions play a relevant role in determining and stabilizing the structures of proteins, and are important in the stabilization of the three-dimensional structures of peptides, and these interactions also play an important part in protein-ligand binding [1–3].

Endomorphin-1 (EM1, H–Tyr–Pro–Trp–Phe–NH_2) and endomorphin-2 (EM2, H–Tyr–Pro–Phe–Phe–NH_2) are endogenous opioid peptides that display high affinity and selectivity for the μ-opioid receptor [4]. Both tetrapeptides contain aromatic amino acids (Tyr, Trp and Phe for EM1, and Tyr and Phe for EM2), which can interact with each other. These aromatic–aromatic interactions between residues with aromatic side-chains can stabilize the different conformers of endomorphins (EMs).

Fiori et al. [5] investigated the preferred conformers of EM1 in aqueous solution and in different micelles. In AOT micelles, their results revealed the close packing of the aromatic side-chains of Tyr^1 and Trp^3 in *cis*-EM1, while this close contact was not observed in *trans*-EM1. They assumed that the interaction between the aromatic side-chains of Tyr^1 and Phe^4 can play a role in the stabilization of the structure of *trans*-EM1 in aqueous solution. In et al. [6] observed close contact between the side-chains of Tyr^1 and Phe^4 in the conformers with a folded backbone in EM2-OH, and also found structures in which the side-chains of Tyr^1 and Phe^3 were close to each other.

C–H···π-interactions can occur between a C–H-donor group and a π-acceptor group in proteins and peptides, and are characterized as weak H-bonds. These interactions play an important role in the stabilization of protein structures and their secondary structural elements, and are relevant in protein–protein and protein-peptide interactions and in molecular recognition [7,8].

One type of C–H···π-interactions is the interplay between a Pro and an aromatic amino acid in peptides and proteins. C–H···π-interactions formed between neighboring side-chains of Pro and an aromatic amino acid can stabilize the *cis*

* Corresponding author. Tel.: +36 62 599 600; fax: +36 62 433 133.
E-mail address: leitgeb@nucleus.szbk.u-szeged.hu (B. Leitgeb).

0223-5234/$ - see front matter © 2005 Elsevier SAS. All rights reserved.
doi:10.1016/j.ejmech.2004.10.015

peptide bond [9,10]. The proline–aromatic interactions may also be important in the stabilization of the structure of β-turns [8]. From an investigation of six residue peptides, Yao et al. [11,12] concluded that in peptides containing the Aro-*cis*-Pro–Aro motif (Aro is an aromatic amino acid), the aromatic side-chains are packed against the Pro ring, and these proline–aromatic stacking interactions are important in the stabilization of the structure of the type VI turn. For the *cis*-Aro–Pro peptide bond, Pal and Chakrabarti [10] reported that the C–H···π-interactions between the Pro and the preceding or following aromatic amino acid can stabilize the structure of the type VI turn.

Both opioid tetrapeptides contain Pro in position 2 and aromatic amino acids in positions 1, 3 and 4. Pro can interact with these amino acids with aromatic side-chain, and these proline–aromatic interactions can stabilize the different conformers of EMs.

A compact sandwich structure was earlier observed in *cis*-EM1, in which the aromatic rings of Tyr^1 and Trp^3 were packed against Pro^2, whereas in *trans*-EM1 this compact structure was not found [5,13]. Podlogar et al. [13] detected this conformation with stacking of the Tyr^1, Pro^2 and Trp^3 rings only in DMSO; in the course of a molecular dynamics simulation in aqueous solution, this conformational feature of *cis*-EM1 was not observed. For *trans*-[D-Pro^2]EM1, Paterlini et al. [14] performed simulated annealing calculations using NMR restraints and molecular dynamics simulations, and also observed a compact structure created by the packing of the side-chains of Tyr^1 and Trp^3 around Pro^2. Similarly as for *cis*-EM1, the side-chain packing interactions were also found in *cis*-EM2, where the aromatic rings of Tyr^1 and Phe^3 were packed against the Pro^2 ring [6].

In the present study, we investigated the aromatic–aromatic interactions between different aromatic amino acids, and the interactions between Pro^2 and the aromatic amino acids in the conformers obtained by random searches for all four types (*cis* or *trans* and charged or uncharged) of EM1 and EM2. For all types of interacting aromatic–aromatic and proline–aromatic pairs, the various geometric orientations were determined and the rotamers of the side-chains of the aromatic amino acids were identified. We examined the aromatic–aromatic and proline–aromatic interactions in the preferred secondary structures (β-turns, N-terminal inverse γ-turns, C-terminal γ-turns and C-terminal inverse γ-turns).

2. Materials and methods

2.1. Random search

Random searches were carried out with SYBYL 6.9 software (Tripos Incorporated, St. Louis, MO) on an Origin2000 workstation running the Irix 6.5 operation system (Silicon Graphics, Inc.).

EM1 and EM2 were modeled in the neutral (NH_2–) and charged (NH_3^+–) forms of the N-terminal amino group, and random searches were performed with *cis* and *trans* Tyr^1–Pro^2 peptide bonds. Thus, depending on the ionization state of the N-terminal amino group and the *cis* or *trans* nature of the Tyr^1–Pro^2 peptide bond, four separate random searches were carried out for both EM1 and EM2.

For energy calculations, the AMBER all-atom force field [15] was applied with the use of the distance-dependent dielectric constant ($\epsilon = 4.5r$) to simulate the effect of water, and a 15 Å cut-off was applied for non-bonding interactions. The starting structures with an extended peptide backbone were minimized in three steps by using three different minimization procedures successively. First, the steepest descent method was applied; the conjugated gradient algorithm followed; and finally a modified Newton method (Broyden-Fletcher-Goldfarb-Shanno, BFGS) was used; the convergence criteria were 100, 1 and 0.01 kcal mol^{-1} $Å^{-1}$, respectively, on the gradient.

After the three-step minimization procedure, random searches were performed; all rotatable torsion angles of the backbone and side-chains were included in the conformational search. For all four types of EM1 and EM2, random searches with 40 000 iterations were carried out. A relative energy cut-off value of 7 kcal mol^{-1} was used and the root-mean-square (RMS) threshold was set at 0.2 Å. The chirality was checked to avoid inversion of the chiral centers. Energy minimization was performed by means of the Powell conjugated gradient method on each conformation generated by random searches. The maximum number of iterations was set at 10 000, and a convergence criterion of 0.005 kcal mol^{-1} $Å^{-1}$ was applied on the gradient.

For *trans*-H_2N-EM1, *cis*-H_2N-EM1, *trans*-H_3N^+-EM1 and *cis*-H_3N^+-EM1, the numbers of conformers generated by random searches were 985, 514, 739 and 544, respectively. For *trans*-H_2N-EM2, *cis*-H_2N-EM2, *trans*-H_3N^+-EM2 and *cis*-H_3N^+-EM2, the numbers of conformers obtained by random searches were 988, 766, 998 and 529, respectively.

2.2. Aromatic–aromatic interactions

To investigate the aromatic–aromatic interactions in both tetrapeptides, the centroids of the side-chain rings of aromatic amino acids were determined, and the pairwise distances between these centroids were calculated. For both Tyr and Phe, the six-membered phenyl ring was used to determine their centroids, and for Trp, both the five- and six-membered rings of the indole group were used, separately. Centroids are the centers of the five- or six-membered rings of the side-chains of aromatic amino acids. For EM1, the aromatic rings of the side-chains of Tyr, Trp and Phe were labeled as Tyr^1, $Trp(5)^3$, $Trp(6)^3$ and Phe^4, respectively, according to the sequence number of these amino acids in the tetrapeptide (Trp(5) indicates the five-membered ring and Trp(6) the six-membered ring of the side-chain of Trp). For EM2, the aromatic rings of the side-chains of Tyr and two Phe-s were labeled in the same way, as Tyr^1, Phe^3 and Phe^4, respectively.

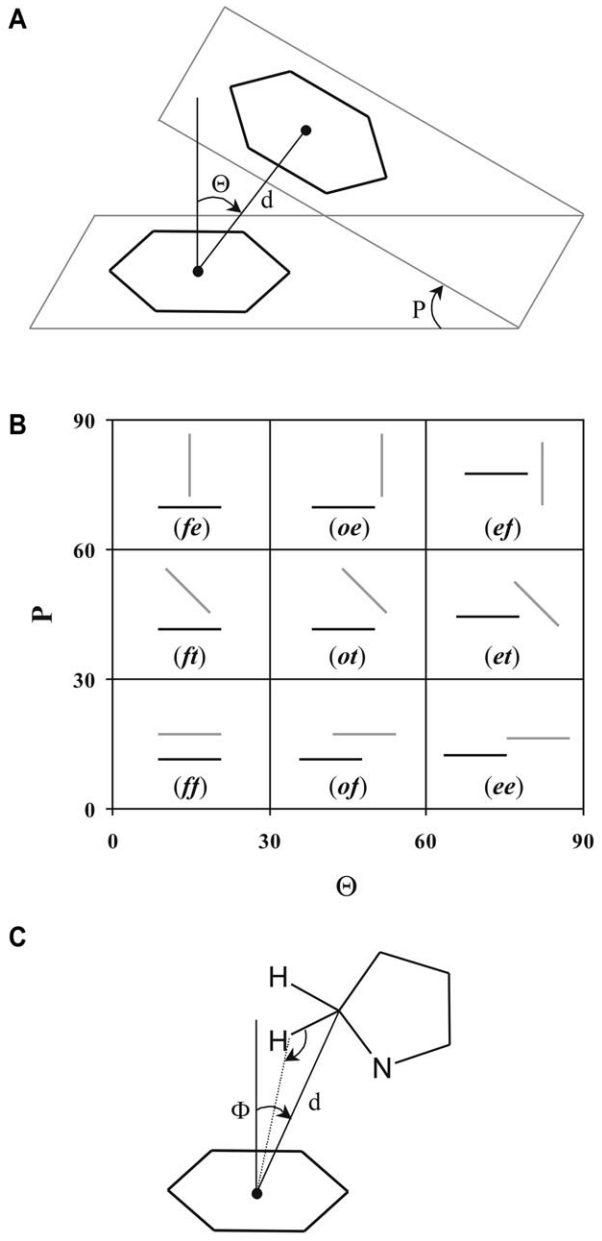

Fig. 1. (A) Three parameters (d, P and θ) used to investigate the aromatic–aromatic interactions. d is the distance between the side-chain centroids, P is the interplanar angle between two rings, θ is the angle between the line joining the centroids of the two interacting aromatic rings and the normal to the plane of the reference ring. (For proline–aromatic interactions, P is the interplanar angle between the pyrrolidine ring and the aromatic ring, θ is the angle between the line joining the centroids of the Pro and aromatic rings and the normal to the plane of the pyrrolidine ring).
(B) Various geometric orientations of the aromatic–aromatic and proline–aromatic interactions in accordance with the different combinations of P and θ. For aromatic–aromatic interactions, the black line indicates the plane of the aromatic ring of the reference residue and the grey line indicates the plane of the aromatic ring of the second residue in the interacting pair. For proline–aromatic interactions, the black line indicates the plane of the pyrrolidine ring of Pro and the grey line indicates the plane of the ring of the aromatic amino acid in the interacting pair.
(C) Different criteria used in the determination of the proline–aromatic interactions. d is the distance between the carbon atom of the pyrrolidine ring of Pro[2] and the centroid of the aromatic ring, Φ is the angle between the line joining the carbon atom of Pro[2] to the centroid of the aromatic ring and the normal to the plane of the aromatic ring, C–H····centroid is the angle subtended at the hydrogen atom by the bond to the carbon atom and the line joining the hydrogen atom and the centroid of the aromatic ring.

The pairwise distances (d) between the side-chain centroids were measured, and an aromatic–aromatic interaction was assumed to exist if the distance between two centroids was less than 5.5 Å.

To determine the geometric orientations of the interacting aromatic side-chains, two parameters were calculated, as described by Burley and Petsko [2]; Bhattacharyya et al. [16]. One of these is the interplanar angle (P) between two rings. For Tyr, Trp(6) and Phe, the planes were determined by the six-membered rings, and for Trp(5) by the five-membered ring. The other parameter is the angle (θ) between the line joining the centroids of the two interacting aromatic rings and the normal to the plane of the reference ring. The normal passes through the centroid of the aromatic ring. The reference residue is the first aromatic amino acid in the sequence. The three parameters (d, P and θ) used to investigate the aromatic–aromatic interactions are presented in Fig. 1A.

The relative spatial orientations of the interacting aromatic rings were characterized on the basis of the two parameters (P and θ), as described by Bhattacharyya et al. [16]. The various types of aromatic–aromatic interactions are classified in accordance with the different combinations of P and θ in Fig. 1B. On the basis of the two angles, nine different geometric orientations of the interacting rings can be distinguished, which are indicated by two letters: *ff*, *of*, *ee*, *ft*, *ot*, *et*, *fe*, *oe* and *ef*. The first letter relates to the reference residue and shows whether this ring interacts with its face (*f*) or edge (*e*), or the centroid of the second ring is in an offset (*o*) position. The second letter relates to the second ring in the interacting pair and shows whether this ring is tilted (*t*) relative to the reference ring, or takes part in the aromatic–aromatic interaction with its face (*f*) or edge (*e*).

This classification of the nine geometries corresponds to the other nomenclature of the aromatic–aromatic interactions [17]: the *ff*, *of* and *ee* orientations correspond to the fully stacking or face-to-face, staggered stacking and parallel in-plane interactions, respectively; the *ft*, *ot* and *et* orientations correspond to the tilted interactions; and the *fe* and *ef* orientations correspond to the edge-to-face or T-shaped geometry, and the *oe* orientation to the cogwheel or L-shaped geometry.

2.3. Proline–aromatic interactions

To investigate the proline–aromatic interactions in both tetrapeptides, the centroids of the Pro ring and the side-chain rings of the aromatic amino acids were determined. For Pro, the five-membered pyrrolidine ring was used to determine its centroid, which is the center of the pyrrolidine ring. For the aromatic amino acids, centroids were determined as described above. For both EM1 and EM2, the Pro ring was labeled as

Pro^2, according to its sequence number in the tetrapeptides, and the aromatic rings of the side-chains of different aromatic amino acids were labeled in the same way as described previously.

In the determination of the proline–aromatic interactions, the distances (d) between any carbon atom of the pyrrolidine ring of Pro^2 and the centroids of the aromatic rings were first measured. The angle (Φ) between the line joining the carbon atom of Pro^2 to the centroid of the aromatic ring and the normal to the plane of the aromatic ring was then calculated. The normal passes through the centroid of the aromatic ring. Furthermore, the angle subtended at the hydrogen atom by the bond to the carbon atom and the line joining the hydrogen atom and the centroid of the aromatic ring was measured. To determine the proline–aromatic interactions, the following criteria were applied. If the distance between any carbon atom of the Pro^2 ring and the centroid of the aromatic ring was within 4.5 Å [9], if the value of Φ was smaller than 30°, and finally if the angle centered at the hydrogen atom was greater than 120° [8], we assumed the interaction to be a proline–aromatic interaction. The criteria used in the determination of the proline–aromatic interactions are given in Fig. 1C.

To determine the geometric orientations of the proline–aromatic interactions, two parameters (the interplanar angle, P, and θ) were calculated as for the aromatic–aromatic interactions (see Fig. 1A), and as described by Bhattacharyya and Chakrabarti [8]. For Pro, the plane was determined by the five-membered pyrrolidine ring, and for the aromatic amino acids, by the appropriate five- or six-membered rings of the side-chains. In this case, the reference residue was Pro for all proline–aromatic interactions, and thus θ was determined as the angle between the line joining the centroids of the Pro and aromatic rings and the normal to the plane of the pyrrolidine ring. The normal passes through the centroid of the Pro ring.

To characterize the relative spatial orientations of the interacting Pro and aromatic rings, the same grid composed of nine elements was applied as for the aromatic–aromatic interactions, and as described by Bhattacharyya et al. [8,16]. On the basis of the two parameters (P and θ), nine types of geometric orientations of the proline–aromatic interactions can be distinguished: *ff*, *of*, *ee*, *ft*, *ot*, *et*, *fe*, *oe*, and *ef* geometries, as shown in Fig. 1B. The first letter relates to the Pro^2, and the second letter to the interacting aromatic ring.

3. Results

3.1. Aromatic–aromatic interactions in EM1 and EM2

The numbers of aromatic–aromatic interactions between the side-chains of different aromatic amino acids in the conformers for all four types (*cis* or *trans* and charged or uncharged) of both EM1 and EM2 are shown in Table 1.

For all types of interacting aromatic pairs in *trans*-EMs, larger numbers of aromatic–aromatic interactions were found than in *cis*-EMs. Furthermore, in the neutral and charged forms of *trans*-EM2, the numbers of Tyr^1–Phe^3 and Phe^3–Phe^4 interactions were larger than the number of Tyr^1–Phe^4 interacting pairs. In *trans*-H_3N^+-EM1, similar numbers of Tyr^1–Trp^3, Tyr^1–Phe^4 and Trp^3–Phe^4 interactions were observed, while in *trans*-H_2N-EM1, the number of Trp^3–Phe^4 interacting pairs was lower than that in *trans*-H_3N^+-EM1.

Depending on whether $Trp(5)^3$ or $Trp(6)^3$ was used to define the aromatic–aromatic interactions, different numbers of such interactions were observed in all four types of EM1. For the neutral and charged forms of *trans*-EM1, the number of Tyr^1–$Trp(5)^3$ interactions was larger than the number of Tyr^1–$Trp(6)^3$ interacting pairs, while for the neutral and charged forms of *cis*-EM1, the relationship between the Tyr^1–$Trp(5)^3$ and Tyr^1–$Trp(6)^3$ interactions was the opposite. For all four types of EM1, the number of $Trp(5)^3$–Phe^4 interactions was larger than the number of $Trp(6)^3$–Phe^4 interacting pairs. In spite of the differences, for 56–88% of Tyr^1–$Trp(5)^3$ and $Trp(5)^3$–Phe^4 interactions, the distance of the centroid of $Trp(6)^3$ from the centroid of the interacting aromatic ring was within 5.5 Å, and for 56–92% of Tyr^1–$Trp(6)^3$ and $Trp(6)^3$–Phe^4 interactions, the distance between the centroid of $Trp(5)^3$ and the centroid of the other aromatic ring was also within the cut-off distance of 5.5 Å.

The numbers of different orientations of the various interacting aromatic pairs in the conformers for all four types (*cis* or *trans* and charged or uncharged) of EM1 and EM2 are presented in Tables 2 and 3.

Table 1
Numbers of aromatic–aromatic interactions between the side-chains of different aromatic amino acids in the conformers for all four types (*cis* or *trans* and charged or uncharged) of EM1 and EM2

	trans-H_2N-EM1	*cis*-H_2N-EM1	*trans*-H_3N^+-EM1	*cis*-H_3N^+-EM1
Tyr^1–$Trp(5)^3$	396 (40)[a]	70 (14)	248 (34)	158 (29)
Tyr^1–$Trp(6)^3$	301 (31)	99 (19)	225 (30)	183 (34)
Tyr^1–Phe^4	181 (18)	80 (16)	135 (18)	60 (11)
$Trp(5)^3$–Phe^4	128 (13)	110 (21)	291 (39)	91 (17)
$Trp(6)^3$–Phe^4	114 (12)	68 (13)	279 (38)	75 (14)
	trans-H_2N-EM2	*cis*-H_2N-EM2	*trans*-H_3N^+-EM2	*cis*-H_3N^+-EM2
Tyr^1–Phe^3	306 (31)	106 (14)	356 (36)	118 (22)
Tyr^1–Phe^4	165 (17)	131 (17)	157 (16)	51 (10)
Phe^3–Phe^4	278 (28)	134 (17)	263 (26)	59 (11)

[a] The numbers in brackets are the ratios of the conformers containing aromatic–aromatic interactions (in %) relative to the total numbers of conformers.

Table 2
Numbers of different orientations of Tyr^1–$Trp(5)^3$, Tyr^1–$Trp(6)^3$, Tyr^1–Phe^4, $Trp(5)^3$–Phe^4 and $Trp(6)^3$–Phe^4 interacting aromatic pairs in the conformers for all four types (*cis* or *trans* and charged or uncharged) of EM1

trans-H_2N-EM1			*cis*-H_2N-EM1			*trans*-H_3N^+-EM1			*cis*-H_3N^+-EM1		
Tyr^1–$Trp(5)^3$											
9	43	33	–	1	18	–	7	13	–	4	22
58	87	65	37	–	–	11	24	28	115	7	–
11	90	–	11	3	–	2	161	2	4	6	–
Tyr^1–$Trp(6)^3$											
11	9	32	1	3	20	6	4	8	–	6	14
49	78	32	42	7	13	12	22	15	128	13	7
19	50	21	7	6	–	45	102	11	5	10	–
Tyr^1–Phe^4											
7	35	45	22	19	3	1	21	23	15	25	2
16	12	20	16	7	–	29	12	30	6	–	–
11	35	–	5	8	–	9	10	–	1	11	–
$Trp(5)^3$–Phe^4											
11	–	11	12	6	9	4	4	12	12	4	8
15	31	2	3	36	11	27	112	9	5	28	5
53	5	–	25	8	–	106	17	–	15	14	–
$Trp(6)^3$–Phe^4											
8	2	8	8	1	3	11	1	3	6	1	2
17	20	2	4	13	6	44	92	3	7	26	2
38	19	–	27	6	–	88	37	–	29	2	–

Table 3
Numbers of different orientations of Tyr^1–Phe^3, Tyr^1–Phe^4 and Phe^3–Phe^4 interacting aromatic pairs in the conformers for all four types (*cis* or *trans* and charged or uncharged) of EM2

trans-H_2N-EM2			*cis*-H_2N-EM2			*trans*-H_3N^+-EM2			*cis*-H_3N^+-EM2		
Tyr^1–Phe^3											
4	12	47	1	1	23	10	17	71	–	2	22
27	37	26	70	–	–	102	24	47	94	–	–
16	134	3	11	–	–	3	76	6	–	–	–
Tyr^1–Phe^4											
7	27	38	18	12	4	3	19	36	9	3	6
16	14	31	50	20	2	21	16	21	10	–	1
16	15	1	6	19	–	12	27	2	4	18	–
Phe^3–Phe^4											
66	4	56	31	2	38	61	2	73	14	9	14
36	31	10	13	12	13	27	23	9	2	3	3
51	24	–	11	14	–	54	14	–	1	13	–

For Tyr^1–$Trp(5)^3$ and Tyr^1–$Trp(6)^3$ interactions in *trans*-H_2N-EM1 and for Tyr^1–Phe^3 interactions in the neutral and charged forms of *trans*-EM2, the distributions of the different geometric orientations in the grid composed of nine elements were approximately the same. In this case, the preferred geometries were the staggered stacking (*of*), the different types of tilted orientations (*ft*, *ot* and *et*) and *ef* (see Fig. 2A–E). For Tyr^1–$Trp(5)^3$ and Tyr^1–$Trp(6)^3$ interactions in *trans*-H_3N^+-EM1, different distributions were observed, and the predominant orientation was the staggered stacking (*of*). In *cis*-EMs, the predominant geometry was *ft* (see Fig. 2F), and the numbers of this orientation were higher in the charged forms than in the neutral forms of *cis*-EMs.

For Tyr^1–Phe^4 interactions in all four types of EM1 and EM2, the distributions of the various geometries in the grid were somewhat different.

In the neutral and charged forms of *trans*-EM1, the distributions of $Trp(5)^3$–Phe^4 and $Trp(6)^3$–Phe^4 interactions differed from those of Phe^3–Phe^4 interactions in the neutral and charged forms of *trans*-EM2. For the former, the predominant geometries were the fully stacking (*ff*) and *ot*, while for the latter, mainly fully stacking (*ff*) and two types of edge-to-face (*fe* and *ef*) orientations were observed (see Fig. 3). In the cases of *cis*-EM1 and *cis*-EM2, the distributions also differed. In the neutral and charged forms of *cis*-EM1, the preferred geometries were the fully stacking (*ff*) and *ot*, whereas in the neutral and charged forms of *cis*-EM2, mainly edge-to-face (*fe* and *ef*) orientations were found.

In all four types of EM1 and EM2, conformers were observed which contain two different interacting aromatic pairs simultaneously. For the neutral and charged forms of *trans*-EMs, the numbers of different combinations of the aro-

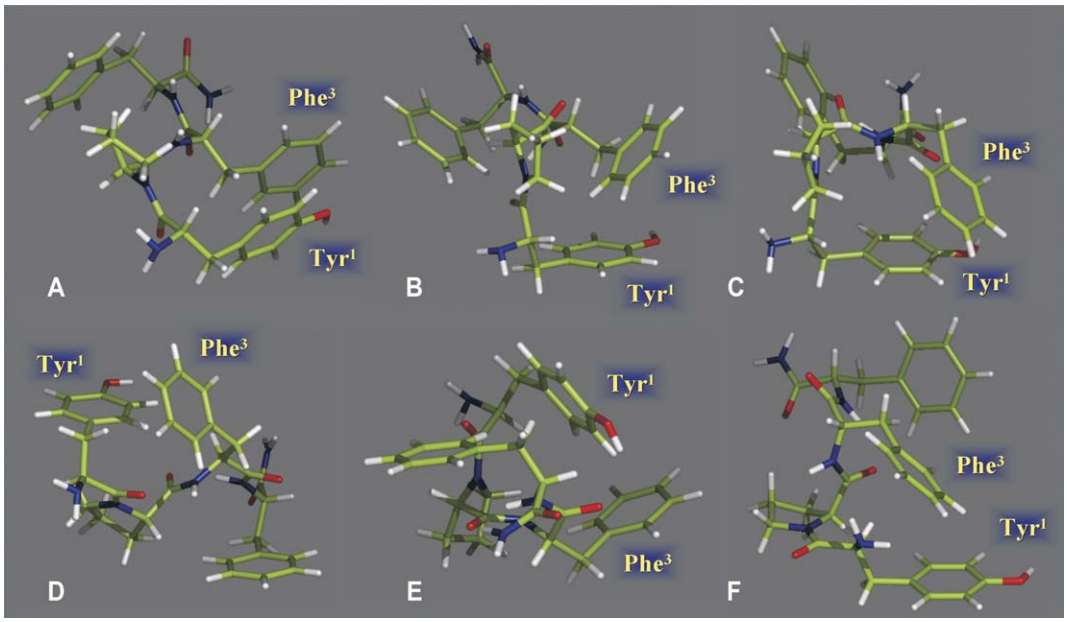

Fig. 2. Preferred geometric orientations of Tyr^1–Trp^3 and Tyr^1–Phe^3 interactions in EM1 and EM2. The *of* (A), *ft* (B), *ot* (C), *et* (D) and *ef* (E) geometries for Tyr^1–Phe^3 interactions in *trans*-H_2N-EM2, and the *ft* (F) geometry for Tyr^1–Phe^3 interactions in *cis*-H_2N-EM2.

matic–aromatic interactions were higher than for the neutral and charged forms of *cis*-EMs. For *trans*-EMs, the proportions of conformers containing two different interacting aromatic pairs were between 10% and 14% of the total numbers of conformers, while for *cis*-EMs, these proportions were between 2% and 4% of the total numbers of conformers. In the conformers possessing two different interacting aromatic pairs, various spatial arrangements of the aromatic side-chains were observed, in accordance with the different geometric orientations and various rotamer combinations. The number of conformers in which all three aromatic amino acids take part in the same aromatic–aromatic interactions at the same time was very small.

3.2. Rotamer combinations of the side-chains in aromatic–aromatic interactions

The proportions of various rotamer combinations of the aromatic side-chains in the different aromatic–aromatic interactions in the conformers for all four types (*cis* or *trans* and charged or uncharged) of EM1 and EM2 are given in Tables 4 and 5. For the rotamer combinations, the first rota-

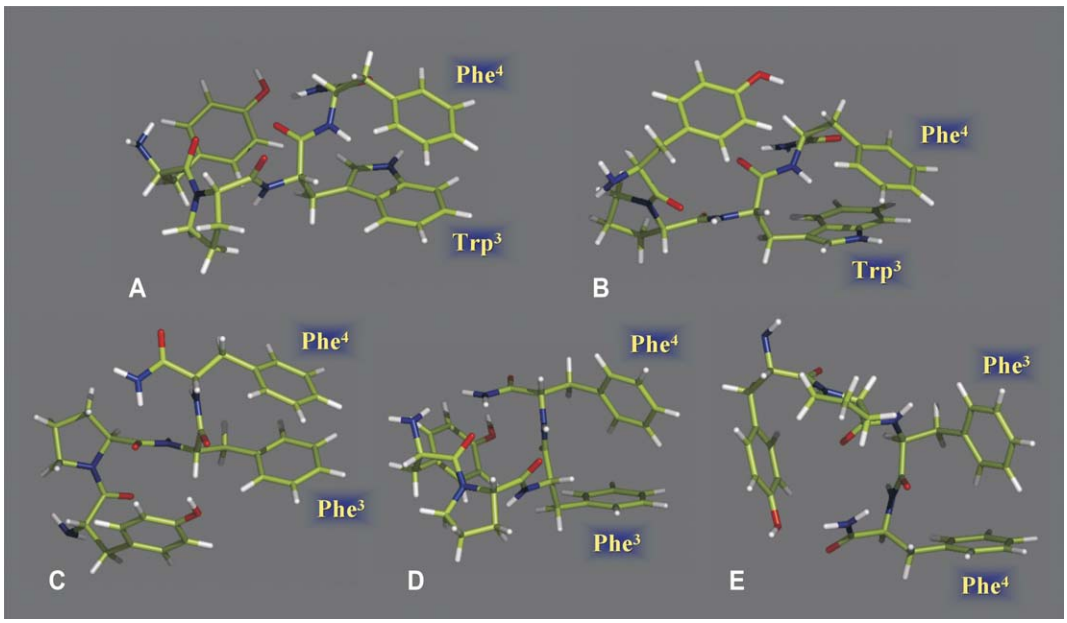

Fig. 3. Preferred geometric orientations of Trp^3–Phe^4 and Phe^3–Phe^4 interactions in EM1 and EM2. The *ff* (A) and *ot* (B) geometries for Trp^3–Phe^4 interactions in *trans*-H_2N-EM1, and the *ff* (C), *fe* (D) and *ef* (E) geometries for Phe^3–Phe^4 interactions in *trans*-H_2N-EM2.

Table 4
Proportions (in %) of various rotamer-combinations of the aromatic side-chains in the different aromatic–aromatic interactions in the conformers for all four types (*cis* or *trans* and charged or uncharged) of EM1

trans-H_2N-EM1		*cis*-H_2N-EM1		*trans*-H_3N^+-EM1		*cis*-H_3N^+-EM1	
Tyr^1–$Trp(5)^3$							
trans–*g*(–)[a]	70.7	*g*(–)–*g*(–)	54.3	*g*(+)–*g*(+)	35.9	*g*(–)–*g*(–)	63.9
trans–*trans*	14.1	*trans*–*g*(–)	27.1	*g*(–)–*g*(+)	19.4	*g*(+)–*g*(+)	19.0
trans–*g*(+)	5.6	*g*(+)–*g*(+)	18.6	*g*(+)–*trans*	15.3	*trans*–*g*(–)	13.3
g(–)–*g*(–)	3.8			*trans*–*trans*	9.3	*g*(–)–*g*(+)	3.8
g(+)–*g*(+)	2.3			*g*(–)–*g*(–)	6.9		
g(+)–*g*(–)	1.5			*g*(+)–*g*(–)	6.4		
g(+)–*trans*	1.3			*trans*–*g*(–)	4.8		
g(–)–*g*(+)	0.7			*trans*–*g*(+)	2.0		
Tyr^1–$Trp(6)^3$							
trans–*g*(–)	66.4	*g*(–)–*g*(–)	39.4	*g*(+)–*g*(+)	40.0	*g*(–)–*g*(–)	59.0
trans–*trans*	13.2	*trans*–*g*(–)	36.4	*g*(–)–*g*(+)	22.2	*g*(+)–*g*(+)	20.8
trans–*g*(+)	6.3	*g*(+)–*g*(+)	21.2	*g*(+)–*trans*	8.9	*trans*–*g*(–)	14.8
g(–)–*g*(–)	4.7	*g*(–)–*trans*	2.0	*trans*–*trans*	8.0	*g*(–)–*g*(+)	3.8
g(+)–*g*(+)	3.0	*trans*–*g*(+)	1.0	*g*(–)–*g*(–)	7.6	*g*(+)–*g*(–)	1.6
g(+)–*g*(–)	2.7			*g*(+)–*g*(–)	5.8		
g(–)–*g*(+)	2.0			*trans*–*g*(–)	4.4		
g(+)–*trans*	1.7			*trans*–*g*(+)	3.1		
Tyr^1–Phe^4							
trans–*g*(–)	68.5	*g*(–)–*g*(–)	51.3	*g*(+)–*g*(–)	60.0	*g*(–)–*g*(–)	33.2
g(+)–*g*(–)	8.8	*trans*–*g*(–)	13.7	*trans*–*g*(–)	25.9	*g*(+)–*g*(–)	16.7
trans–*g*(+)	8.8	*g*(–)–*g*(+)	12.5	*trans*–*g*(+)	4.5	*g*(+)–*g*(+)	13.3
g(–)–*g*(–)	5.0	*g*(–)–*trans*	11.2	*g*(+)–*g*(+)	3.0	*g*(–)–*g*(+)	11.7
trans–*trans*	3.9	*trans*–*g*(+)	5.0	*g*(–)–*g*(–)	2.2	*g*(–)–*trans*	11.7
g(–)–*g*(+)	3.3	*g*(+)–*g*(+)	3.8	*g*(–)–*g*(+)	2.2	*trans*–*g*(–)	10.0
g(+)–*trans*	1.1	*g*(+)–*g*(–)	2.5	*g*(+)–*trans*	2.2	*g*(+)–*trans*	1.7
g(+)–*g*(+)	0.6					*trans*–*g*(+)	1.7
$Trp(5)^3$–Phe^4							
trans–*g*(–)	79.7	*trans*–*g*(–)	46.4	*trans*–*g*(–)	47.8	*g*(+)–*g*(–)	48.4
g(+)–*g*(–)	12.5	*g*(+)–*g*(–)	28.1	*trans*–*g*(+)	33.7	*trans*–*g*(+)	25.2
trans–*g*(+)	5.5	*g*(+)–*g*(+)	21.0	*g*(+)–*g*(–)	18.2	*g*(+)–*g*(+)	22.0
g(+)–*g*(+)	2.3	*trans*–*g*(+)	4.5	*g*(+)–*g*(+)	0.3	*trans*–*g*(–)	4.4
$Trp(6)^3$–Phe^4							
trans–*g*(–)	80.7	*trans*–*g*(–)	47.1	*trans*–*g*(–)	52.0	*g*(+)–*g*(–)	44.0
g(+)–*g*(–)	8.8	*g*(+)–*g*(–)	28.0	*trans*–*g*(+)	35.8	*trans*–*g*(+)	30.7
trans–*g*(+)	7.0	*g*(+)–*g*(+)	17.6	*g*(+)–*g*(–)	12.2	*g*(+)–*g*(+)	17.3
g(+)–*g*(+)	3.5	*trans*–*g*(+)	7.3			*trans*–*g*(–)	8.0

[a] For the rotamer combinations, the first rotamer relates to the side-chain of the reference residue and the second rotamer to the side-chain of the interacting residue.

mer relates to the side-chain of the reference residue and the second rotamer to the side-chain of the interacting residue.

For Tyr^1–$Trp(5)^3$ and Tyr^1–$Trp(6)^3$ interactions in the neutral and charged forms of *trans*-EM1, for Tyr^1–Phe^3 interactions in *trans*-H_2N-EM2 and *trans*-H_3N^+-EM2, and for Tyr^1–Phe^4 interactions in all four types of EM1 and EM2, many more different kinds of rotamer combinations were observed as compared with those for Tyr^1–$Trp(5)^3$ and Tyr^1–$Trp(6)^3$ interactions in the neutral and charged forms of *cis*-EM1, for Tyr^1–Phe^3 interactions in *cis*-H_2N-EM2 and *cis*-H_3N^+-EM2, for $Trp(5)^3$–Phe^4 and $Trp(6)^3$–Phe^4 interactions in all four types of EM1 and for Phe^3–Phe^4 interactions in the neutral and charged forms of both *cis*- and *trans*-EM2. In the two latter cases, only four side-chain combinations were found (except for $Trp(6)^3$–Phe^4 interactions in *trans*-H_3N^+-EM1, where one of these was absent): *g*(+)–*g*(–), *g*(+)–*g*(+), *trans*–*g*(–) and *trans*–*g*(+). For all types of aromatic–aromatic interactions, one, two or a few large populations of rotamer combinations were found.

If we select the mostly populated rotamer combination for all four types of EM1 and EM2, the following can be observed. For all types of aromatic–aromatic interactions in the neutral form of *trans*-EMs, the predominant side-chain pair was *trans*–*g*(–). For Tyr^1–Phe^4 and Trp^3–Phe^4 or Phe^3–Phe^4 interactions in the charged form of *trans*-EMs, the mainly populated combinations were *g*(+)–*g*(–) and *trans*–*g*(–), respectively. For Tyr^1–Trp^3, Ty^1–Phe^3 and Tyr^1–Phe^4 interactions in the neutral and charged forms of *cis*-EMs, mostly the *g*(–)–*g*(–) rotamer combination was preferred.

Table 5
Proportions (in %) of various rotamer-combinations of the aromatic side-chains in the different aromatic–aromatic interactions in the conformers for all four types (*cis* or *trans* and charged or uncharged) of EM2

trans-H_2N-EM2		*cis*-H_2N-EM2		*trans*-H_3N^+-EM2		*cis*-H_3N^+-EM2	
Tyr^1–Phe^3							
trans–*g*(–)[a]	31.4	*g*(–)–*g*(–)	75.5	*g*(+)–*g*(–)	27.8	*g*(–)–*g*(–)	78.0
trans–*trans*	21.6	*trans*–*g*(–)	21.7	*trans*–*g*(–)	26.4	*trans*–*g*(–)	20.3
trans–*g*(+)	18.6	*g*(+)–*g*(+)	1.9	*g*(+)–*g*(+)	14.3	*g*(+)–*g*(+)	1.7
g(–)–*g*(+)	16.7	*g*(–)–*g*(+)	0.9	*g*(+)–*trans*	10.1		
g(+)–*g*(+)	7.7			*g*(–)–*g*(+)	8.7		
g(+)–*trans*	2.3			*trans*–*g*(+)	6.5		
g(–)–*g*(–)	1.0			*g*(–)–*g*(–)	4.5		
g(+)–*g*(–)	0.7			*trans*–*trans*	1.7		
Tyr^1–Phe^4							
trans–*g*(–)	52.1	*g*(–)–*g*(–)	40.5	*g*(+)–*g*(–)	34.4	*g*(–)–*g*(–)	33.2
trans–*g*(+)	18.2	*g*(–)–*trans*	22.1	*trans*–*g*(–)	30.6	*g*(–)–*trans*	27.5
g(+)–*g*(–)	17.6	*g*(–)–*g*(+)	18.3	*g*(+)–*g*(+)	13.4	*g*(–)–*g*(+)	25.5
g(–)–*g*(+)	4.2	*g*(+)–*g*(+)	6.1	*g*(–)–*g*(–)	6.4	*trans*–*g*(–)	5.9
g(–)–*g*(–)	3.0	*g*(+)–*g*(–)	3.8	*g*(+)–*trans*	5.7	*g*(+)–*g*(+)	3.9
trans–*trans*	2.4	*trans*–*g*(–)	3.8	*trans*–*g*(+)	4.5	*g*(+)–*g*(–)	2.0
g(+)–*g*(+)	1.8	*trans*–*g*(+)	3.1	*g*(–)–*g*(+)	3.8	*trans*–*g*(+)	2.0
g(+)–*trans*	0.7	*g*(+)–*trans*	2.3	*g*(–)–*trans*	0.6		
				trans–*trans*	0.6		
Phe^3–Phe^4							
trans–*g*(–)	38.8	*g*(+)–*g*(–)	32.1	*trans*–*g*(–)	49.8	*g*(+)–*g*(+)	44.1
trans–*g*(+)	21.9	*g*(+)–*g*(+)	32.1	*g*(+)–*g*(+)	20.9	*g*(+)–*g*(–)	35.5
g(+)–*g*(+)	19.8	*trans*–*g*(–)	28.4	*g*(+)–*g*(–)	17.9	*trans*–*g*(–)	11.9
g(+)–*g*(–)	19.5	*trans*–*g*(+)	7.4	*trans*–*g*(+)	11.4	*trans*–*g*(+)	8.5

[a] For the rotamer combinations, the first rotamer relates to the side-chain of the reference residue and the second rotamer to the side-chain of the interacting residue.

3.3. Aromatic–aromatic interactions in the secondary structures

In the course of our previous conformational analyses of EMs, we investigated the preferred secondary structures in the conformers of both EM1 and EM2 [18,19]. In the determination of the β-turns, the same ranges of the torsion angles Φ_2, Ψ_2, Φ_3 and Ψ_3 were applied as previously [20,21]. In this case, to determine the γ-turns and inverse γ-turns, the following torsion angle ranges were used: for the γ-turns $70° < \Phi_3 < 95°$ and $-75° < \Psi_3 < -45°$, for the N-terminal inverse γ-turns $-95° < \Phi_2 < -70°$ and $45° < \Psi_2 < 75°$, and for the C-terminal inverse γ-turns $-95° < \Phi_3 < -70°$ and $45° < \Psi_3 < 75°$ [22–24]. The numbers of different types of β-turns and γ-turns in the conformers for all four types of EM1 and EM2 are shown in Table 6.

In the neutral forms of EMs, significant numbers of type III β-turns were found, while in the charged forms of EMs, the numbers of these β-turns were smaller. In the neutral and charged forms of *trans*-EMs, type V β-turns were observed

Table 6
Numbers of different types of β-turns and γ-turns in the conformers for all four types (*cis* or *trans* and charged or uncharged) of EM1 and EM2

	trans-H_2N-EM1	*cis*-H_2N-EM1	*trans*-H_3N^+-EM1	*cis*-H_3N^+-EM1
β-turns				
Type III	152	108	73	34
Type V	58	–	14	–
γ-turns				
N-terminal inverse γ-turn	193	–	39	–
C-terminal γ-turn	124	36	16	18
C-terminal inverse γ-turn	108	61	64	42
	trans-H_2N-EM2	*cis*-H_2N-EM2	*trans*-H_3N^+-EM2	*cis*-H_3N^+-EM2
β-turns				
Type III	106	180	66	46
Type V	33	–	13	–
γ-turns				
N-terminal inverse γ-turn	135	–	78	–
C-terminal γ-turn	83	81	110	32
C-terminal inverse γ-turn	91	80	115	42

Table 7
Numbers of proline–aromatic interactions between Pro^2 and the side-chains of different aromatic amino acids in the conformers for all four types (*cis* or *trans* and charged or uncharged) of EM1 and EM2

	trans-H_2N-EM1	*cis*-H_2N-EM1	*trans*-H_3N^+-EM1	*cis*-H_3N^+-EM1
Pro^2–Tyr^1	139 (14)[a]	267 (52)	96 (13)	181 (33)
Pro^2–$Trp(5)^3$	123 (12)	55 (11)	13 (2)	35 (6)
Pro^2–$Trp(6)^3$	191 (19)	107 (21)	35 (5)	85 (16)
Pro^2–Phe^4	121 (12)	77 (15)	19 (3)	75 (14)
	trans-H_2N-EM2	*cis*-H_2N-EM2	*trans*-H_3N^+-EM2	*cis*-H_3N^+-EM2
Pro^2–Tyr^1	146 (15)	293 (38)	181 (18)	252 (48)
Pro^2–Phe^3	86 (9)	152 (20)	98 (10)	67 (13)
Pro^2–Phe^4	80 (8)	101 (13)	117 (12)	99 (19)

[a] The numbers in brackets are the ratios of the conformers containing proline–aromatic interactions (in %) relative to the total numbers of conformers.

and inverse γ-turns were also found in the N-terminal tripeptide fragments (Tyr^1–Pro^2–Trp^3 and Tyr^1–Pro^2–Phe^3), whereas in the neutral and charged forms of *cis*-EMs, type V β-turns and N-terminal inverse γ-turns were completely absent. In the charged forms of *trans*-EMs, the numbers of these β-turns and inverse γ-turns were lower than in the neutral forms of *trans*-EMs. In all four types of EM1 and EM2, different numbers of γ-turns and inverse γ-turns were found in the C-terminal tripeptide fragments (Pro^2–Trp^3–Phe^4 and Pro^2–Phe^3–Phe^4). Our previous conformational analyses of EMs demonstrated approximately similar proportions of different types of β-turns and γ-turns [18,19].

In the present conformational study, several conformers were observed which contain an N-terminal inverse γ-turn and a C-terminal γ-turn or inverse γ-turn simultaneously. Of course, these multiple turns were found only in the conformers of *trans*-EMs, because inverse γ-turns in the N-terminal tripeptide fragments are not present in the conformers of *cis*-EMs. Few of the structures in which an inverse γ-turn is located in the N-terminal fragment and a γ-turn is also located in the C-terminal fragment simultaneously contain a type V β-turn. The reason for this is that the ranges of the torsion angles Φ_2, Ψ_2, Φ_3 and Ψ_3 for the type V β-turn overlap with the ranges of the torsion angles Φ_2 and Ψ_2 for the N-terminal inverse γ-turn, and Φ_3 and Ψ_3 for the C-terminal γ-turn.

For the neutral and charged forms of *trans*-EMs, significant numbers of Tyr^1–Trp^3 and Tyr^1–Phe^3 interactions were found in the type III β-turns, while the type V β-turns contained mainly Trp^3–Phe^4 and Phe^3–Phe^4 interacting pairs, and in these turns Tyr^1–Trp^3 and Tyr^1–Phe^3 interactions were completely absent. In the conformers possessing N-terminal inverse γ-turns, all types of aromatic–aromatic interactions were observed; nevertheless, these structures included mostly Tyr^1–Trp^3, Tyr^1–Phe^3, Trp^3–Phe^4 and Phe^3–Phe^4 interacting pairs. In the conformers containing C-terminal γ-turns, significant numbers of Tyr^1–Trp^3 interactions were found for *trans*-H_2N-EM1, while mainly Tyr^1–Phe^4 and Phe^3–Phe^4 interacting pairs were observed for *trans*-H_2N-EM2, and predominantly Tyr^1–Phe^3 and Tyr^1–Phe^4 interactions were found for *trans*-H_3N^+-EM2. In the conformers possessing C-terminal inverse γ-turns, great proportions of Tyr^1–Trp^3 and Tyr^1–Phe^3 interacting pairs were observed.

For *cis*-H_2N-EM1 and *cis*-H_2N-EM2, significant numbers of Tyr^1–Phe^4, $Trp(5)^3$–Phe^4 and Phe^3–Phe^4 interactions were found in the type III β-turns, while for *cis*-H_3N^+-EM1 and *cis*-H_3N^+-EM2 these β-turns contained mainly $Trp(5)^3$–Phe^4 and Phe^3–Phe^4 interacting pairs. For the neutral and charged forms of *cis*-EM2, Tyr^1–Phe^3 interactions were not present in the type III β-turns. In the conformers possessing C-terminal γ-turns, mainly Tyr^1–Trp^3 and $Trp(5)^3$–Phe^4 interacting pairs were found for *cis*-H_2N-EM1, while mostly Tyr^1–Phe^3 interactions were observed for the neutral and charged forms of *cis*-EM2. In the conformers containing C-terminal inverse γ-turns, mainly Tyr^1–Trp^3, Tyr^1–Phe^3 and Tyr^1–Phe^4 interacting pairs were found for *cis*-H_2N-EM1 and *cis*-H_2N-EM2, whereas predominantly Tyr^1–Trp^3 and Tyr^1–Phe^3 interactions were observed for *cis*-H_3N^+-EM1 and *cis*-H_3N^+-EM2.

These results revealed that the majority of the different types of β-turns and γ-turns contain one of the different aromatic–aromatic interactions. For the neutral and charged forms of *trans*-EMs, more interacting aromatic pairs were observed in the secondary structures than for the neutral and charged forms of *cis*-EMs.

3.4. Proline–aromatic interactions in EM1 and EM2

The numbers of proline–aromatic interactions between Pro^2 and the side-chains of different aromatic amino acids in the conformers for all four types (*cis* or *trans* and charged or uncharged) of both EM1 and EM2 are presented in Table 7.

For Pro^2–Tyr^1 interactions in *cis*-EMs, larger numbers of proline–aromatic interactions were found than in *trans*-EMs. Furthermore, in all four types of EM2, the number of Pro^2–Tyr^1 interactions was larger in comparison with the numbers of Pro^2–Phe^3 and Pro^2–Phe^4 interacting pairs. In *trans*-H_3N^+-EM1 and in the neutral and charged forms of *cis*-EM1, similar proportions of proline–aromatic interactions were observed, while in *trans*-H_2N-EM1, the number of Pro^2–$Trp(6)^3$ interacting pairs was larger, but the numbers of Pro^2–$Trp(5)^3$ and Pro^2–Phe^4 interactions were lower than that of Pro^2–Tyr^1 interactions.

Depending on whether $Trp(5)^3$ or $Trp(6)^3$ was used to define the proline–aromatic interactions, different numbers of such interactions were observed in all four types of EM1.

For the neutral and charged forms of *cis*- and *trans*-EM1, the number of Pro^2–$Trp(6)^3$ interactions was larger than the number of Pro^2–$Trp(5)^3$ interacting pairs. In spite of the differences, for 74–89% of Pro^2–$Trp(5)^3$ interactions, $Trp(6)^3$ also participated in the proline–aromatic interactions, and for 29–47% of Pro^2–$Trp(6)^3$ interactions, $Trp(5)^3$ also took part in the proline–aromatic interactions.

For Pro^2–Tyr^1 interactions in the neutral and charged forms of *trans*-EM1 and *trans*-EM2, only C^δ of the Pro^2 ring was involved in the C–H····π-interactions, while in the neutral and charged forms of *cis*-EM1 and *cis*-EM2, predominantly C^α of the pyrrolidine ring took part in the proline–aromatic interactions, but C^β and C^γ were also observed in smaller numbers.

For Pro^2–$Trp(5)^3$, Pro^2–$Trp(6)^3$ and Pro^2–Phe^3 interactions in the neutral and charged forms of *trans*-EM1 and *trans*-EM2, mainly C^β and C^γ of the Pro^2 ring joined in the C–H····π-interactions, whereas in the neutral and charged forms of *cis*-EM1 and *cis*-EM2, especially C^β, C^γ and C^δ of the pyrrolidine ring participated in the proline–aromatic interactions.

For Pro^2–Phe^4 interactions in the neutral and charged forms of *trans*-EM1 and *trans*-EM2, mostly C^α and C^β of the Pro^2 ring took part in the C–H····π-interactions, while in the neutral and charged forms of *cis*-EM1 and *cis*-EM2, principally C^β and C^γ of the pyrrolidine ring were involved in the proline–aromatic interactions.

The numbers of different orientations of the various interacting proline–aromatic pairs in the conformers for all four types (*cis* or *trans* and charged or uncharged) of EM1 and EM2 are given in Tables 8 and 9.

For Pro^2–Tyr^1 interactions in the neutral and charged forms of *trans*-EMs, the predominant orientation was *ot*, while in the neutral and charged forms of *cis*-EMs, the preferred geometries were *ff* and *ot* (see Fig. 4A, B). Bhattacharyya and Chakrabarti [8] also observed that the preferred orientation between the Pro ring and the preceding aromatic ring was *ot*.

For Pro^2–$Trp(6)^3$ interactions in all four types of EM1, significant amounts of the *of* and *ot* geometries were observed (see Fig. 4C, D), whereas for Pro^2–Phe^3 interactions in all four types of EM2, the preferred orientation was *of*. Bhattacharyya and Chakrabarti [8] also found that the predominant geometry between the Pro ring and the following aromatic ring was *of*.

Table 8
Numbers of different orientations of Pro^2–Tyr^1, Pro^2–$Trp(5)^3$, Pro^2–$Trp(6)^3$ and Pro^2–Phe^4 interacting pairs in the conformers for all four types (*cis* or *trans* and charged or uncharged) of EM1

trans-H_2N-EM1			*cis*-H_2N-EM1			*trans*-H_3N^+-EM1			*cis*-H_3N^+-EM1		
Pro^2–Tyr^1											
–	18	–	–	–	–	–	8	–	–	–	–
–	121	–	13	168	–	–	88	–	2	145	–
–	–	–	82	4	–	–	–	–	33	1	–
Pro^2–$Trp(5)^3$											
–	–	1	–	–	–	–	–	–	–	–	–
21	21	–	18	11	–	–	4	–	–	4	–
47	33	–	4	22	–	3	6	–	19	12	–
Pro^2–$Trp(6)^3$											
–	–	2	–	–	–	–	–	4	–	–	1
16	60	8	1	48	4	–	14	–	–	31	1
45	60	–	15	39	–	6	11	–	12	40	–
Pro^2–Phe^4											
–	14	40	–	5	29	–	2	9	–	1	31
19	42	3	10	11	3	–	6	2	14	8	1
2	1	–	18	1	–	–	–	–	18	2	–

Table 9
Numbers of different orientations of Pro^2–Tyr^1, Pro^2–Phe^3 and Pro^2–Phe^4 interacting pairs in the conformers for all four types (*cis* or *trans* and charged or uncharged) of EM2

trans-H_2N-EM2			*cis*-H_2N-EM2			*trans*-H_3N^+-EM2			*cis*-H_3N^+-EM2		
Pro^2–Tyr^1											
–	16	–	–	–	–	–	18	–	–	–	–
–	129	–	6	234	–	–	163	–	19	167	–
–	1	–	50	3	–	–	–	–	65	1	–
Pro^2–Phe^3											
–	–	–	–	–	–	–	–	–	–	–	–
12	8	–	21	72	1	8	22	–	2	9	–
19	47	–	12	46	–	9	59	–	21	35	–
Pro^2–Phe^4											
–	6	20	–	12	44	–	11	39	–	4	58
6	16	20	16	20	2	3	36	18	9	10	1
7	5	–	4	3	–	7	3	–	17	–	–

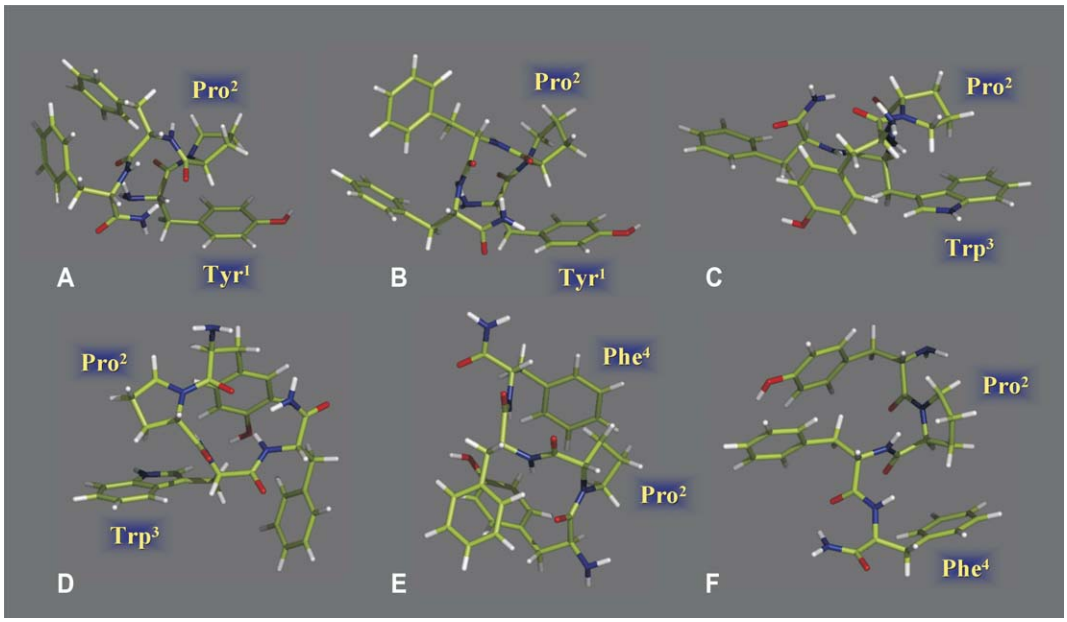

Fig. 4. Preferred geometric orientations of Pro^2–Tyr^1, Pro^2–Trp^3, Pro^2–Phe^3 and Pro^2–Phe^4 interactions in EM1 and EM2. The *ff* (A) and *ot* (B) geometries for Pro^2–Tyr^1 interactions in *cis*-H_2N-EM2, the *of* (C) and *ot* (D) geometries for Pro^2–Trp^3 interactions in *trans*-H_2N-EM1, and the *ot* (E) and *ef* (F) geometries for Pro^2–Phe^4 interactions in *trans*-H_2N-EM2.

For Pro^2–Phe^4 interactions in the neutral and charged forms of *trans*-EMs, significant amounts of the *ot* and *ef* geometries were found (see Fig. 4E, F), while in the neutral and charged forms of *cis*-EMs, the predominant orientation was *ef*.

In all four types of EM1 and EM2, conformers were observed in which Pro^2 interacts with two aromatic amino acids simultaneously. For the neutral and charged forms of *trans*-EMs, the numbers of different combinations of the proline–aromatic interactions were lower than those for the neutral and charged forms of *cis*-EMs. For *trans*-EMs, the proportions of conformers containing two different interacting proline–aromatic pairs were between 2% and 4% of the total numbers of conformers, while for *cis*-EMs, these proportions were between 10% and 20% of the total numbers of conformers. In the conformers possessing two different interacting proline–aromatic pairs, various spatial arrangements of the aromatic side-chains were observed around Pro^2, in accordance with the different geometric orientations.

In the conformers containing Pro^2–Tyr^1 and Pro^2–Trp^3 interacting pairs for *cis*-EM1, and in the conformers possessing Pro^2–Tyr^1 and Pro^2–Phe^3 interacting pairs for *cis*-EM2, in a majority of the cases the compact sandwich structure was observed, in which the aromatic rings of Tyr^1 and Trp^3 were packed against Pro^2 for *cis*-EM1, and the aromatic rings of Tyr^1 and Phe^3 were packed against Pro^2 for *cis*-EM2, as described previously [5,6,13]. In the conformers containing Pro^2–Tyr^1 and Pro^2–Phe^4 interacting pairs for both *cis*-EM1 and *cis*-EM2, the compact sandwich structure in which the aromatic rings of Tyr^1 and Phe^4 were packed against the Pro^2 ring was only found in a few cases.

3.5. Side-chain rotamers of the aromatic amino acids in proline–aromatic interactions

For Pro^2–Tyr^1, Pro^2–$Trp(5)^3$ and Pro^2–Phe^3 interactions in all four types of EM1 and EM2, only one type of side-chain rotamer of the aromatic amino acids was observed, which was *trans* for Tyr^1 and *g*(–) for Trp^3 and Phe^3. For Pro^2–$Trp(6)^3$ and Pro^2–Phe^4 interactions in all four types of EM1 and EM2, predominantly the *g*(–) rotamer of Trp^3 and Phe^4 was found, but a smaller number of the *g*(+) rotamer of these aromatic amino acids was also observed. Of course, the proline–aromatic interaction can only occur between Pro^2 and any aromatic ring if the aromatic amino acids possess the rotamers mentioned above, because only in these cases are the Pro^2 and aromatic rings in close contact.

3.6. Proline–aromatic interactions in the secondary structures

For the neutral and charged forms of *trans*-EMs, significant numbers of Pro^2–$Trp(6)^3$ and Pro^2–Phe^3 interactions were found in the type III β-turns, while the type V β-turns contained mainly Pro^2–Tyr^1 interacting pairs, and in these turns Pro^2–$Trp(5)^3$ and Pro^2–Phe^3 interactions were completely absent. In the conformers possessing N-terminal inverse γ-turns, mostly Pro^2–$Trp(6)^3$ and Pro^2–Phe^4 interacting pairs were observed for *trans*-H_2N-EM1, and Pro^2–Phe^4 interactions for *trans*-H_2N-EM2. In the conformers containing C-terminal γ-turns, significant numbers of Pro^2–Phe^4 interactions were found for *trans*-H_2N-EM1, while mainly Pro^2–Tyr^1 and Pro^2–Phe^3 interacting pairs were observed for the neutral and charged forms of *trans*-EM2. In the conformers

possessing C-terminal inverse γ-turns, all types of proline–aromatic interactions were found; nevertheless, these structures included mostly Pro^2–Trp^3 interacting pairs for *trans*-H_2N-EM1.

For the neutral and charged forms of *cis*-EMs, significant numbers of Pro^2–Tyr^1, Pro^2–Trp^3 and Pro^2–Phe^3 interactions were observed in the type III β-turns. In the conformers containing C-terminal γ-turns or inverse γ-turns, mostly Pro^2–Tyr^1 interacting pairs were found for the neutral and charged forms of *cis*-EM1, while mainly Pro^2–Tyr^1 and Pro^2–Phe^3 interactions were observed for *cis*-H_2N-EM2.

These results revealed that the numbers of proline–aromatic interactions are larger in the different types of β-turns and γ-turns for the neutral and charged forms of *cis*-EMs than in the turn structures for the neutral and charged forms of *trans*-EMs.

3.7. Aromatic–aromatic and proline–aromatic interactions in EM1 and EM2

In all four types of EM1 and EM2, conformers were observed which contain two different interacting aromatic pairs simultaneously, as described previously. Furthermore, conformers were also found in which Pro^2 interacts with two aromatic amino acids simultaneously, as mentioned above. Additionally, conformers were detected which contain one interacting aromatic pair and one proline–aromatic interaction simultaneously. In these conformers possessing simultaneous aromatic–aromatic and proline–aromatic interactions, various spatial arrangements of the side-chains of the aromatic amino acids were observed, in accordance with the different geometric orientations of the aromatic–aromatic and proline–aromatic interactions and the various rotamer combinations of the aromatic side-chains.

4. Discussion and conclusion

Both opioid tetrapeptides contain Pro in position 2, and aromatic amino acids (Tyr, Trp and Phe) in positions 1, 3 and 4, which can interact with each other. These aromatic–aromatic and proline–aromatic interactions can stabilize the different conformers of EM1 and EM2.

In the course of previous investigations of EMs, close contacts between the aromatic side-chains of the different amino acids were observed. These are as follows: the close packing of the side-chains of Tyr^1 and Trp^3 in *cis*-EM1, the interaction between the side-chains of Tyr^1 and Phe^4 in *trans*-EM1 [5], the close packing of the side-chains of Tyr^1 and Phe^3 in EM2-OH and the close contact between the side-chains of Tyr^1 and Phe^4 in EM2-OH with a folded backbone [6]. For *cis*-EMs, a compact sandwich structure was earlier observed, in which the aromatic rings of Tyr^1 and Trp^3 were packed against Pro^2 for *cis*-EM1, and the aromatic rings of Tyr^1 and Phe^3 were packed against Pro^2 for *cis*-EM2 [5,6,13].

We investigated, in detail, the various aromatic–aromatic and proline–aromatic interactions in both tetrapeptides, and different types of such interactions were found: Tyr^1–Trp^3, Tyr^1–Phe^4, Trp^3–Phe^4, Pro^2–Tyr^1, Pro^2–Trp^3 and Pro^2–Phe^4 interacting pairs for EM1, and Tyr^1–Phe^3, Tyr^1–Phe^4, Phe^3–Phe^4, Pro^2–Tyr^1, Pro^2–Phe^3 and Pro^2–Phe^4 interacting pairs for EM2. Compared with the earlier observations, we found more different kinds of aromatic–aromatic and proline–aromatic interactions for both *cis*- and *trans*-EMs. For all types of interacting aromatic pairs, larger numbers of aromatic–aromatic interactions were observed in *trans*-EMs than in *cis*-EMs. Furthermore, in *trans*-EMs (with the exception of *trans*-H_2N-EM1), the numbers of Tyr^1–Trp^3, Tyr^1–Phe^3, Trp^3–Phe^4 and Phe^3–Phe^4 interactions were larger than the number of Tyr^1–Phe^4 interacting pairs. For Pro^2–Tyr^1 interactions in *cis*-EMs, larger numbers of proline–aromatic interactions were found than in *trans*-EMs. Furthermore, in all four types of EMs (with the exception of *trans*-H_2N-EM1), the number of Pro^2–Tyr^1 interactions was larger in comparison with the numbers of Pro^2–Phe^3, Pro^2–Trp^3 and Pro^2–Phe^4 interacting pairs.

For these highly flexible tetrapeptides, three pharmacophore elements have been identified so far: the N-terminal amino group, the Tyr in position 1 and a further aromatic amino acid (Trp or Phe) in position 3 or 4 [5,13]. These results reveal that the aromatic amino acids rank among the putative pharmacophore elements of EM1 and EM2, thus their relative spatial arrangement is important in the binding to the receptor. In the structures stabilized by an aromatic–aromatic or proline–aromatic interaction, the spatial arrangements of the aromatic amino acids are determined by the different geometric orientations and the various rotamer combinations. For all types of aromatic–aromatic and proline–aromatic interactions, the different geometric orientations were determined and their distribution was represented in a grid composed of nine elements. The preferred orientations were identified for Tyr^1–Trp^3, Tyr^1–Phe^4, Trp^3–Phe^4, Pro^2–Tyr^1, Pro^2–Trp^3 and Pro^2–Phe^4 interacting pairs for EM1, and Tyr^1–Phe^3, Tyr^1–Phe^4, Phe^3–Phe^4, Pro^2–Tyr^1, Pro^2–Phe^3 and Pro^2–Phe^4 interacting pairs for EM2. We examined the various rotamer combinations of the side-chains of aromatic amino acids in the different aromatic–aromatic interactions for all four types of EM1 and EM2. In spite of the great variety of rotamer combinations, few large populations of side-chain pairs were observed for all types of interacting aromatic pairs.

As mentioned above, aromatic–aromatic interactions play a relevant role in the stabilization of the three-dimensional structures of peptides [1–3]. Random searches resulted in a great variety of extended and bent structures for all four types of EM1 and EM2. For *trans*-EMs, the number of different aromatic–aromatic interactions showed that the majority of the conformers contained one of the various interacting aromatic pairs. For *cis*-EMs, the numbers of conformers possessing one of the different aromatic–aromatic interactions were lower. The abundance of interacting aromatic pairs implies that the aromatic–aromatic interactions may be important in determining and stabilizing the different conformers of EMs. As mentioned previously, proline–aromatic interactions play

a role in the stabilization of the *cis* peptide bond and the structure of the β-turns [8–10]. The investigation of the proline–aromatic interactions resulted in larger numbers of Pro^2–Tyr^1 interactions for *cis*-EMs than for *trans*-EMs. These results revealed that Pro^2–Tyr^1 interacting pairs may contribute to the stability of *cis* peptide bond in these tetrapeptides.

In the conformers generated by random searches for all four types of EM1 and EM2, different types of β-turns and γ-turns were observed. In the neutral and charged forms of *trans*-EM1 and *trans*-EM2, types III and V β-turns were found, as well as inverse γ-turns located in the N-terminal tripeptide fragment. In the neutral and charged forms of *cis*-EM1 and *cis*-EM2, type III β-turns were also observed, but type V β-turns and N-terminal inverse γ-turns were absent. In all four types of EM1 and EM2, γ-turns and inverse γ-turns were found in the C-terminal tripeptide fragment.

In our previous conformational analyses of EM1 and EM2, we investigated, in detail, the intramolecular H-bonds in the conformers obtained by simulated annealing [18,19]. The results showed that the different secondary structures are stabilized by intramolecular H-bonds and bifurcated H-bonds between backbone atoms. The β-turns are stabilized by 1 ← 4 H-bonds, the N-terminal inverse γ-turns by 1 ← 3 H-bonds, and the C-terminal γ-turns and inverse γ-turns by 2 ← 4 H-bonds. Further H-bonds were also observed which can stabilize the different bent structures. Although the different intramolecular H-bonds stabilize the various structures of EM1 and EM2, other interactions (i.e. aromatic–aromatic and proline–aromatic interactions) may contribute to the stability of the conformers of these tetrapeptides. We investigated the various aromatic–aromatic and proline–aromatic interactions in the different types of β-turns and γ-turns for all four types of EM1 and EM2. These results revealed that the majority of the different types of β-turns and γ-turns contained one of the various interacting aromatic–aromatic or proline–aromatic pairs. In the turn structures with intramolecular H-bonds, the aromatic–aromatic and proline–aromatic interactions can produce a further stabilizing effect. In our previous conformational studies, however, β-turns were also detected which satisfied the Φ and Ψ criteria, but which lacked stabilizing H-bonds. In the turn structures without intramolecular H-bonds, the aromatic–aromatic and proline–aromatic interactions can play an important role in the stabilization of the three-dimensional structures of conformers.

On the basis of the present results, it can be assumed that a conformation stabilized by an aromatic–aromatic or proline–aromatic interaction may be important in the association with the receptor and in ligand recognition. Determination of the importance of aromatic–aromatic or proline–aromatic interactions in the receptor-ligand binding requires detailed exploration of the binding site of the μ-opioid receptor and the joint investigation of the receptor and its ligands.

Acknowledgements

This research was supported by grants NKFP 1/27/2001 and OTKA M045378.

References

[1] S.K. Burley, G.A. Petsko, Science 229 (1985) 23–28.
[2] S.K. Burley, G.A. Petsko, Adv. Protein Chem. 39 (1988) 125–189.
[3] M.L. Waters, Curr. Opin. Chem. Biol. 6 (2002) 736–741.
[4] J.E. Zadina, L. Hackler, L.J. Ge, A.J. Kastin, Nature 386 (1997) 499–502.
[5] S. Fiori, C. Renner, J. Cramer, S. Pegoraro, L. Moroder, J. Mol. Biol. 291 (1999) 163–175.
[6] Y. In, K. Minoura, H. Ohishi, H. Minakata, M. Kamigauchi, M. Sugiura, et al., J. Pept. Res. 58 (2001) 399–412.
[7] M. Nishio, Y. Umezawa, M. Hirota, Y. Takeuchi, Tetrahedron 51 (32) (1995) 8665–8701.
[8] R. Bhattacharyya, P. Chakrabarti, J. Mol. Biol. 331 (2003) 925–940.
[9] M. Brandl, M.S. Weiss, A. Jabs, J. Sühnel, R. Hilgenfeld, J. Mol. Biol. 307 (2001) 357–377.
[10] D. Pal, P. Chakrabarti, J. Mol. Biol. 294 (1999) 271–288.
[11] J. Yao, V.A. Feher, B.F. Espejo, M.T. Raymond, P.E. Wright, H.J. Dyson, J. Mol. Biol. 243 (1994) 736–753.
[12] J. Yao, H.J. Dyson, P.E. Wright, J. Mol. Biol. 243 (1994) 754–766.
[13] B.L. Podlogar, G. Paterlini, D.M. Ferguson, G.C. Leo, D.A. Demeter, F.K. Brown, et al., FEBS Lett. 439 (1998) 13–20.
[14] M.G. Paterlini, F. Avitabile, B.G. Ostrowski, D.M. Ferguson, P.S. Portoghese, Biophys. J. 78 (2000) 590–599.
[15] W.D. Cornell, P. Cieplak, C.I. Bayly, I.R. Gould, K.M. Merz, D.M. Ferguson, et al., J. Am. Chem. Soc. 117 (1995) 5179–5197.
[16] R. Bhattacharyya, U. Samanta, P. Chakrabarti, Protein Eng. 15 (2) (2002) 91–100.
[17] J. Singh, J.M. Thornton, FEBS Lett. 191 (1) (1985) 1–6.
[18] B. Leitgeb, F. Ötvös, G. Tóth, Biopolymers 68 (4) (2003) 497–511.
[19] B. Leitgeb, A. Szekeres, G. Tóth, J. Pept. Res. 62 (4) (2003) 145–157.
[20] C. Venkatachalam, Biopolymers 6 (1968) 1425–1436.
[21] P. Lewis, F. Momany, H. Sheraga, Biochim. Biophys. Acta 303 (2) (1973) 211–229.
[22] I. Alkorta, M.L. Suarez, R. Herranz, R.G. Muniz, M.T. Garcia-López, J. Mol. Model. (Online) 2 (1996) 16–25.
[23] E.J. Milner-White, B.M. Ross, R. Ismail, K. Belhadj-Mostefa, R. Poet, J. Mol. Biol. 204 (1988) 777–782.
[24] E.J. Milner-White, J. Mol. Biol. 216 (1990) 385–397.